Abdominal Radiology (2019) 44:3388–3397
https://doi.org/10.1007/s00261-019-02097-x

PELVIS

T2 hyperintense myometrial tumors: can MRI features differentiate leiomyomas from leiomyosarcomas?

Gisela Rio[1] · Mariana Lima[2] · Rui Gil[2] · Mariana Horta[2] · Teresa Margarida Cunha[2]

Published online: 27 June 2019
© Springer Science+Business Media, LLC, part of Springer Nature 2019

Abstract

Purpose To establish MRI features that help differentiate atypical leiomyomas and leiomyomas with degeneration that show hyperintensity on T2WI from leiomyosarcomas.

Methods and materials This retrospective study evaluated 41 women who performed MRI before undergoing hysterectomy and had histologically proven atypical leiomyomas, leiomyomas with degeneration or leiomyosarcomas (21 leiomyomas; 20 leiomyosarcomas); only patients with T2 hyperintense myometrial tumors were included. The association between MRI features (contours; free pelvic fluid; intra-tumoral hemorrhagic areas, T2 heterogeneity; T2 dark areas; flow voids; restriction on diffusion-weighted images; signal intensity and heterogeneity after contrast administration; unenhanced areas, localization of unenhanced areas; necrosis; cystic areas) and the histology (leiomyoma vs. leiomyosarcoma) were calculated using Fisher's exact test. For those features that showed a significant association, a univariate linear regression was performed.

Results Five MRI features demonstrated a significant correlation with malignant histology: irregular borders ($p = 0.03$); "T2 dark" areas ($p = 0.02$); presence of central necrosis ($p = 0.01$); presence of high signal on b1000 DWI ($p < 0.001$); ADC value lower than 0.82×10^{-3} mm^2/s; hyperenhancement of the tumor relative to the myometrium on post-contrast images ($p = 0.02$); and type 3 enhancing curve on DCE. Two of these features demonstrated a significant result predicting a malignant histology: lobulated contours and central necrosis [$F(3;34) = 8{,}95$; $p < 0.001$; $R^2 = 0.506$].

Conclusion The presence of lobulated borders, T2 dark areas, necrosis, hyperintensity relative to the myometrium after contrast administration, central necrosis, presence of high signal on b1000 DWI, ADC value lower than 0.82×10^{-3} mm^2/s and type 3 enhancing curve on DCE can help distinguish between leiomyoma and leiomyosarcoma. The association of lobulated borders and central necrosis can help predict a malignant histology.

Keywords Atypical leiomyomas · Leiomyoma variants · Leiomyosarcomas · Leiomyomas with degeneration · MRI

Introduction

Uterine leiomyomas are a benign entity representing the most common gynecologic neoplasm with a prevalence estimated in 20–40% [1, 2]. On the other hand, leiomyosarcomas (LMS) are rare tumors with aggressive behavior and an incidence of 1.7 in 100,000 women [3]. Distinction between leiomyomas and leiomyosarcomas can be challenging on magnetic resonance imaging (MRI), particularly in the presence of early-stage leiomyosarcomas, leiomyomas with degeneration or variant subtypes of leiomyomas that may demonstrate atypical features on MRI, such as hyperintensity on T2 [4, 5] (Table 1).

As leiomyomas affect mostly women in reproductive age, new conservative treatments, such as uterine artery embolization (UAE) or hormonal therapy, have gained

✉ Gisela Rio
giselario_123@hotmail.com

Mariana Lima
mariana_talina@hotmail.com

Rui Gil
ruitiagogil@gmail.com

Mariana Horta
mariana_horta@hotmail.com

Teresa Margarida Cunha
tmargarida@gmail.com

[1] Hospital de Braga, Oporto, Portugal

[2] Instituto Português de Oncologia de Lisboa Francisco Gentil, Lisbon, Portugal

Table 1 Histological subtypes of leiomyomas included

Uterine leiomyomas showing hyperintensity on T2-WI
Leiomyoma with degeneration:
Cystic
Myxoid
Hemorrhagic
Hydropic
Fatty (lipoleiomyoma)
Leiomyoma variants
Mitotically active
Cellular
Atypical
STUMP

wider acceptance [1]. Therefore, MRI arises as an essential imaging technique in the workup of female patients that are undergoing any of the new treatments, in order to confirm the benignity of the lesions and to diagnose, map, and characterize leiomyomas [6]. Hence, it is essential that the radiologist is aware of the clinical, imaging, and pathological features that help differentiate leiomyoma variants and leiomyomas with degeneration from leiomyosarcomas, since all of them might demonstrate hyperintensity on T2-weighted images [7].

Despite this being a current problem, there are few studies in the literature regarding the value of MRI qualitative features in order to differentiate LMS from atypical leiomyomas (ALM) [8–14]. In addition, most of these studies had a small number of patients with LMS because of their rareness [8–14]; also they grouped LMS, endometrial stromal sarcomas, and carcinosarcomas all in the same category, despite of their very different MRI features and clinical outcomes [8, 11, 12, 14–16]. Our study has the advantage of selecting patients with tumors that show more than 50% areas of T2 hyperintensity (excluding patients that demonstrate more or equal than 50% of hypointensity on T2), which to our knowledge was never used as a criterion before. In addition, we combined the morphologic features of the tumor with their functional behavior on DWI and perfusion, which was also not evaluated in most of the other studies.

Therefore, the purpose of this retrospective study is to establish MRI features that help differentiate ALM that show hyperintensity on T2WI (such as leiomyoma variants and leiomyomas with degeneration) from LMS.

Materials and methods

This retrospective study was approved and granted a waiver consent by our institution's Human Investigations Committee. It was also performed in accordance with Health Insurance Portability and Accountability Act (HIPAA) guidelines.

Patient selection

We retrospectively searched our institutional database to identify all women with any of this pathologically proven tumors: leiomyosarcoma, smooth muscle tumor of uncertain malignant potential (STUMP), cellular leiomyoma, mitotically active leiomyoma, "atypical" leiomyoma and leiomyomas with either hydropic, myxoid, fatty, cystic or hemorrhagic changes. This search found 136 patients with surgically resected myometrial masses or hysterectomy between March 2009 and September 2017.

Only patients who performed MRI 6 months before surgery were included. Furthermore, we only included patients whose tumor MRI showed hyperintensity on T2WI, i.e., tumors constituted by more than 50% of areas of signal intensity higher than that of the myometrium, excluding patients that demonstrate more or equal than 50% of hypointensity on T2. We excluded patients whose exam was obtained without intravenous contrast administration or that didn't cover the whole tumor. The final study population consisted of 41 patients with histopathologically confirmed diagnoses (ALM = 21, LMS = 20)—Fig. 1.

MR imaging protocol

Patients underwent MRI examinations on a 1.5-T scanner (Achieva; Philips, the Netherlands). All patients were examined in the supine position and a phased-array coil was used to perform the body scans. In our hospital T2-weighted images (axial, sagittal, and coronal planes), T1 axial and dynamic perfusion sequences using T1 fat saturated (FS) images were obtained for each patient. The parameters for the Achieva 1.5 T whole-body unit were as follows: repetition time/time-to-echo ratio (TR/TE) 5000/102 ms for T2WI and 500/14 ms for T1WI; matrix size, 512 × 512; section thickness, 4 mm and intersection gap, 0,4 mm. Diffusion -weighted images (DWI) were acquired on an axial plane, using *b* values corresponding to the diffusion-sensitizing gradient of 0, 200, and 1000 s/mm^2, and with single-shot echo-planar imaging sequence (TR/TE) 3100/53 ms, flip angle 90° and matrix size 256 × 256.

Perfusion-weighted images were obtained using a T1 eco-gradient sequence. Five images were acquired after gadolinium was administered. Finally, delayed post-contrast sequence was obtained on axial plane.

Patients fasted for 4–6 h and were then given anti-peristaltic agents to reduce bowel motility.

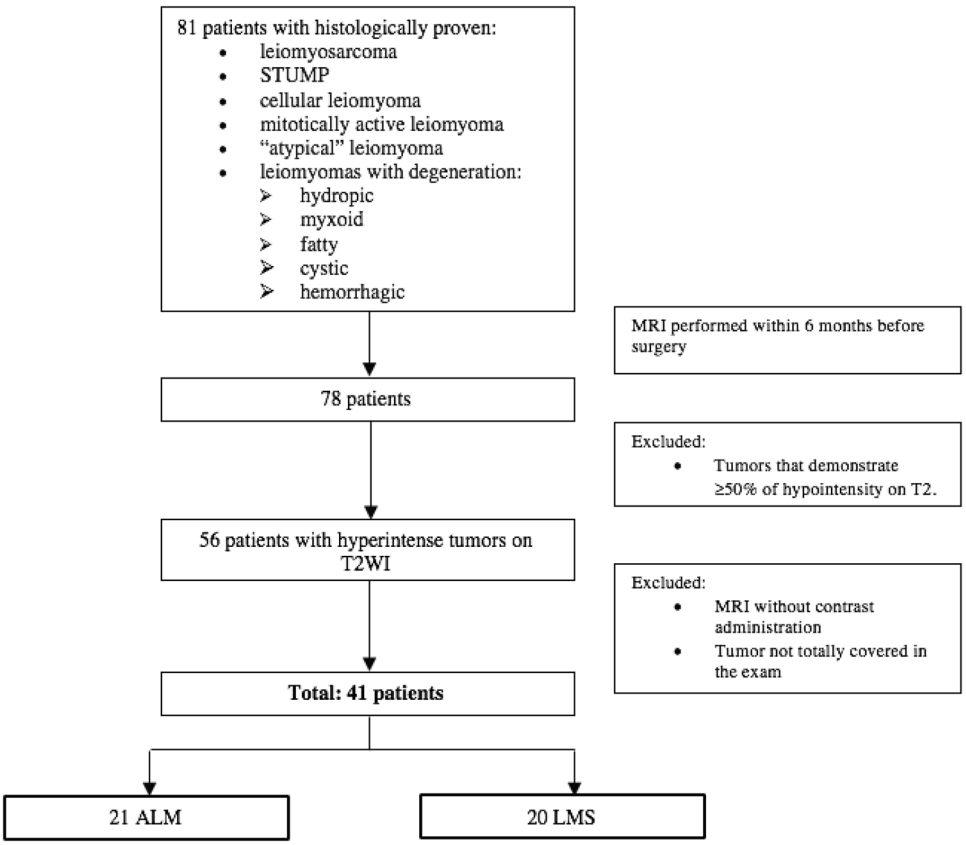

Fig. 1 Patient selection algorithm

Image interpretation

Images were evaluated by a radiologist with 4 years of experience in pelvic MRI; only after this evaluation the collected data were compared with the report of a radiologist specialized in female pelvis (20 years of experience). There was no access to the information about the report and pathology prior to the analysis. In the few cases where the selected features were not described in the report, a third reader was asked to analyze the lacking characteristics.

MRI studies were reviewed and the following features were analyzed (Table 2): size, tumor margin (irregular or smooth), heterogeneity on T2, the presence of intra-tumoral hemorrhage (areas with hyperintensity on T1 defined as any foci brighter than the fat in the pubis at the symphysis), cystic alterations (defined as internal regular foci of T2 signal as bright as fluid in the bladder and of low signal intensity on T1WI), areas of central necrosis (central irregular areas of high T2 lower than the fluid in the bladder and showing lack of enhancement after contrast administration), flow voids (which are seen as dark spots within the vessels representing high flow), T2 dark areas (representing areas of previous hemorrhage that can be seen as areas of signal intensity that are lower than that of muscle). Finally, the presence of pelvic fluid, lymphadenopathies, peritoneal

Table 2 Criteria used for evaluating uterine lesions

MRI features
1. Size
2. Poorly defined margins
3. Areas of intra-tumoral hemorrhage
4. T2 signal heterogeneity
5. Well-defined cystic areas
6. "T2 dark" areas
7. Presence of central necrosis
8. Fluid–fluid levels
9. Flow voids
10. Presence of high signal on b1000 DWI
11. ADC value
12. Heterogeneous enhancement
13. Enhancement of the tumor compared with external myometrium
14. Type of DCE curve
15. Pelvic lymphadenopathy
16. Evidence of peritoneal metastases
17. Invasion of the mass into the bladder, rectum, pelvic side walls, or other structures.
18. Free pelvic fluid

metastases, and invasion of adjacent pelvic organs were evaluated.

A low b1000 signal intensity was defined as a signal equal to that of urine. For diffusion analysis, each reader independently recorded the apparent diffusion coefficient (ADC) values of each tumor by placing the ROIs on ADC maps. The circular ROI was placed to be as large as possible within the limits of the tumors without involving the interface or blood flow. For heterogeneous lesions, care was taken not to involve necrosis, hemorrhagic or cystic space within the lesion by referring to T1- and T2-weighted images.

For perfusion analysis, each reader independently analyzed the dynamic enhancement on a standard workstation, selecting two regions of interest (ROIs), one in the external myometrium and one in the most enhancing part of any solid tissue. The presence of heterogeneous enhancement, avidity of contrast enhancement compared with the external myometrium and the type of enhancing curve on dynamic contrast images were analyzed. We classified the enhancement of the solid tissue using a previously published time intensity curve classification [11].

Statistical analysis

Continuous variables were presented with means and ranges while categorical variables were described with frequencies and percentages. Descriptive analysis was performed using a non-parametric Mann–Whitney test for continuous variables; Fisher's exact test was used for categorical or nominal variables; the association between the later MR and LMS was evaluated using Fisher's exact test.

For those features that demonstrated significant association with the presence of LMS on histology, a univariate analysis was used to predict malignancy.

Inter-reader agreement was assessed with the Cohen's kappa (k) where values between 0 and 0.20 represent slight agreement; 0.21–0.40, fair agreement; 0.41–0.60, moderate agreement; 0.61–0.80, substantial agreement; and 0.81–1.00 almost perfect agreement [17].

A p value of <0.05 was considered to indicate a statistically significant difference.

Statistical analysis was performed using SPSS version 23.0 (SPSS Inc. Chicago, IL, USA).

Results

Patients

There was no statistically difference ($p=0.1$) between mean patient age in the group of ALM (47 years; range 27–59) and the mean patient age in the LMS group (57 years; range 36–71).

The time from MRI to hysterectomy ranged from 12 to 150 days in the cases of LMS with a mean interval of 71 days and 21 to 256 days in the cases of ALM with a mean interval of 86 days.

Patients performed MRI examinations most often for complains of lower abdominal pain/pressure (11/22 in the ALM group and 15/20 in the LMS group) with the majority of the other cases being performed in asymptomatic patients, especially on the ALM group, who performed MRI after the finding of a pelvic mass on ultrasound (8/21 ALM).

We found 20 patients with proven LMS; 16 patients had histologically proven LM with degeneration: three hemorrhagic, four myxoid, seven cystic, and two hydropic and five patients with ALM: one STUMP, three cellular, and one mitotically active.

Patient data are summarized in Table 3.

Qualitative MR imaging features

There was no statistically significant difference ($p=0.48$) in the average size of ALM (mean: 10.2; range 0.65) compared with LMS (mean: 11.3; range: 0.44).

The mean and standard deviation of the ADC value in the ALM (n = 15) were $1.43 \pm 0.21 \times 10^{-3}$ mm^2/s and in the LMS ($n=17$) were $0.82 \pm 0.17 \times 10^{-3}$ mm^2/s.

MRI features that were able to differentiate ALM from LMS for both readers were: (1) irregular borders ($p=0.03$); (2) "T2 dark" areas ($p=0.02$); (3) presence of central necrosis ($p=0,01$); (4) presence of high signal on b1000 DWI (<0.001); (5) ADC value lower than 0.82×10^{-3} mm^2/s; (6) hyperenhancement of the tumor relative to the myometrium on post-contrast images ($p=0.02$); and (7) type 3 enhancing curve on DCE (Fig. 2).

Table 3 Patient data

	ALM ($N=21$)	LMS ($N=20$)
Age (years—mean)	47 (27–59)	57 (36–71)
Menopause status		
Non-menopausal	15	2
Menopausal	6	18
Elevated serum tumor markers		
LDH ≥ 279 U/1 ($N=35$)	9	13
Symptoms		
Asymptomatic	8	4
Menorrhagia/vaginal bleeding	2	1
Abdominal pain	11	15
Time until surgery (days—mean)	86 (21–256)	71 (12–150)
Initial surgery type		
Total hysterectomy	8	20
Myomectomy	12	0

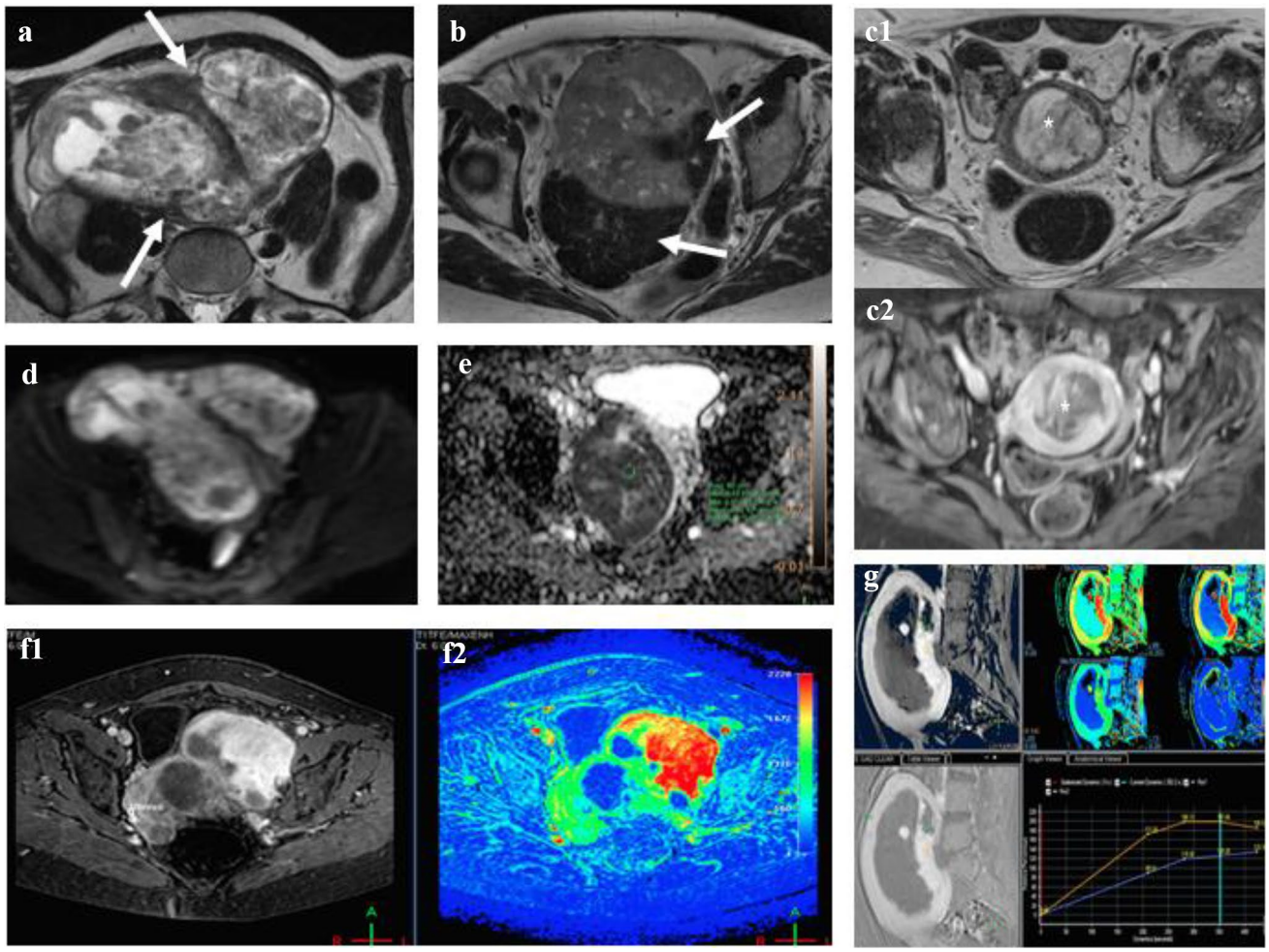

Fig. 2 MRI features that demonstrated the strongest statistical association with LMS at histopathology. Axial T2-weighted image **a** shows a large uterine mass with nodular anterior borders (white arrows); **b** Axial T2-weighted image demonstrates "T2 dark" area in the myometrial mass (white arrow); **c1** T2-weighted image illustrates the presence of central intra-lesioned hyperintense area that doesn't enhance after contrast administration (**c2**), representing necrosis (asterisk). **d** Axial b1000 DWI demonstrates high signal intensity of the tumor; **e** ADC map shows low values within the tumor (white arrow); **f** Axial T1FS after gadolinium administration (**f1**) and the corresponding color mapping (**f2**) show hyperenhancement of the tumor compared with external myometrium; **g** Type III enhancing curve- ROI was placed on the external myometrium and in the most enhancing part of the tumor. The curve demonstrates rapid enhancement of the tumor (red curve) compared with the myometrium (blue curve) and latter washout

For both readers, size, areas of T1 brightness (hemorrhage), T2 heterogeneity; well-defined cystic areas; heterogenous enhancement; fluid–fluid levels; flow voids; type 1 and 2 curves on DCE; pelvic lymphadenopathies; peritoneal metastasis; invasion of pelvic adjacent organs and pelvic fluid did not show statistical significance (Table 4).

Using univariate analysis for the features that showed statistical significance in the differentiation between ALM and LMS, the ones that were predictive of malignancy were found to be the presence of irregular borders (OR = + ∞) and central necrotic areas (OR = + ∞) [$F(3;34) = 8.95$; $p < 0.001$; $R^2 = 0.506$].

Inter-observer agreement

Inter-reader agreement regarding qualitative MRI features ranged between substantial and almost perfect in almost all of the characteristics, except for the presence of lymphadenopathies and the presence of flow voids (Table 5). In particular, agreement levels for tumor margins, intratumoral hemorrhage, central unenhanced area(s), and type of dynamic contrast-enhanced MRI curve were almost perfect.

Table 4 Distribution of MRI features between ALM and LMS

MR findings	ALM ($N=21$)	LMS ($N=20$)	p value	Sensitivity (%)	Specificity (%)
Size	10.2 ± 0.65	11.3 ± 0.44	0.48		
Irregular borders	3	18	**0.01**	90	90
Areas of T1 hyperintensity	2	9	0.35	45	90
T2 heterogeneity	18	17	0.66	85	14
Well defined cystic areas	11	8	0.37	40	47
"T2 dark" areas	3	16	**0.02**	80	85
Heterogeneous enhancement	15	17	0.59	85	28
Presence of central necrosis	3	17	**0.01**	85	85
Fluid–fluid levels	0	2	0.07	10	100
Flow voids	4	5	0.57	25	80
Presence of high signal on b1000 DWI ($N=32$)	3	15	**< 0.001**	93	81
ADC value ($N=32$)	1.43 ± 0.21	0.82 ± 0.17	**0.03**		
Hyperintensity relative to the myometrium post-contrast	5	14	**0.02**	70	76
DCE curve ($N=26$):					
Type 1	4	1	0.06	5	55
Type 2	4	2	0.14	11	55
Type 3	1	14	**0.01**	82	89
Pelvic lymphadenopathy	0	1	0.07	4	100
Evidence of peritoneal metastases	0	1	0.10	4	100
Invasion of the bladder, rectum, pelvic side walls, or other structures	0	1	0.07	4	100
Free pelvic fluid	3	4	0.33	20	86

Bold values are statistically significant

Table 5 Inter-observer agreement

Tumor features	Kappa values (± SD)	Intra-class correlation coefficient
Size		0.953
Tumor margins	0.846 (± 0.10)	
Intra-tumoral hemorrhage	0.862 (± 0.14)	
T2 heterogeneity	0.641 (± 0.12)	
Cystic alterations	0.724 (± 0.16)	
Fluid–fluid levels	0.935 (± 0.06)	
Flow voids		
T2 dark areas	0.733 (± 0.12)	
ADC value		0.876
b1000 signal	0.847 (± 0.14)	
Heterogeneous enhancement	0.735 (± 0.13)	
Central necrosis	0.943 ((± 0.05)	
Type of dynamic contrast-enhanced MRI curve	0.914 (± 0.08)	
Pelvic fluid	0.801 (± 0.13)	
Pelvic metastases	0.657 (± 0.13)	
Lymphadenopathies	0.543 (± 0.14)	
Invasion into the bladder, rectum, pelvic side walls, or other structures	0.812 (± 0.12)	

Discussion

Uterine leiomyomas are the most common uterine tumors and usually affect women in reproductive years [2, 18]. Even though this condition has been the main reason for performing a hysterectomy, many women prefer to be treated using minimally invasive procedures such as leiomyoma morcellation, uterine artery embolization, transvaginal ultrasound-guided radiofrequency myolysis, or MRI-guided focused ultrasound either for preserving fertility or as an alternative to surgery [19, 20]. Even though the prevalence of occult LMS is less than previously estimated (1/8300 hysterectomies), this does not negate the fact that such occult malignancies can and do occur [21]. Therefore, it is of the utmost importance to be able to exclude preoperatively the presence of LMS because these new treatments are contraindicated for malignant tumors in order to avoid intra-abdominal dissemination [22].

The distinction between leiomyomas and LMS cannot be made based on clinical variants [23]. Leiomyomas are much more frequent than LMS, and patients with these conditions tend to present at similar ages and with similar clinical symptoms [24]. While rapid mass enlargement, particularly after menopause, may signify malignancy, it may also be observed with cellular or degenerating leiomyomas [25]. Serum markers such as LDH can be elevated not only with LMS but also with cellular and leiomyomas with degeneration [24].

Hence, imaging, particularly MRI has an essential role in the evaluation of pelvic masses [25].

Most leiomyomas do not create a diagnostic challenge on imaging because of their classic appearance as well demarcated, hypointense masses on T1 and T2WI [26]. LMS, on the other hand, are irregular and ill-defined lesions with intermediate to high signal intensity on T2WI with cystic areas denoting necrosis, scattered hyperintense foci on T1-weighted images, and usually cause massive uterine enlargement [25].

However, leiomyomas with degeneration (which is caused by altered blood supply) and variant subtypes can demonstrate T2 hyperintensity rather than classic hypointensity on T1 and T2WI as well as similar enhancement characteristics as LMS [5, 8]. Therefore, these tumors cause diagnostic misinterpretation and are a challenge in the differentiation with LMS.

It has been suggested that an irregular contour, high signal on T2-WI and hyperintense areas on T1-WI could favor LMS against leiomyoma [8, 9, 27]. Tanaka et al. also proposed that LMS should be considered when there is a combination of these features with non-enhancement following contrast administration [9]. The absence of calcifications was also considered to be related with LMS [5].

Our study evaluated the ability of qualitative MRI features to differentiate LMS from ALM. The qualitative MR features that demonstrated statistical significance in the differentiation between ALM and LMS and were associated with the presence of LMS were: irregular borders ($p = 0.002$); "T2 dark" areas ($p = 0.02$); central necrosis ($p = 0.001$); and ADC value $\leq 0.82 \times 10^{-3}$ m^2/s ($p = 0.03$); presence of high signal on b1000 DWI ($p < 0.001$); hyperintensity relative to the myometrium after contrast administration ($p = 0.02$) and type 3 DCE curve ($p = 0.01$).

Similarly to Lakhman et al., Thomassin-Naggara et al., Sahdev et al., Schwartz et al., and Tanaka et al., we also found that LMS appeared as large masses with irregular borders, and central unenhanced areas on contrast-enhanced images representing necrosis [5, 9, 13–15]. Assuming that a combination of T1 and T2 hyperintensity and unenhanced areas signified malignancy, Tanaka et al. achieved moderate sensitivity (73%) and high specificity (100%) in differentiating benign and malignant smooth muscle tumors [9] and Lakhman et al. higher sensitivity (95–100%) and similarly high specificity (95–100%) for distinguishing LMS from ALM by using the presence of ≥ 3 features to diagnose LMS [13]. Contrary to the literature, we didn't attain statistical significance for the presence of areas of hyperintensity on T1WI (representing areas of hemorrhage), either because we didn't find them in many patient with proven LMS and also because two of our patients with histologically proven leiomyomas had hemorrhagic degeneration, resulting in a sensitivity of 45% but a specificity of 90% for this imaging feature. However, in patients with myometrial tumors that demonstrated hyperintensity on T2WI, we achieved a sensitivity and specificity of 85–90% when combining these features with the presence of irregular borders and central necrosis for the diagnosis of LMS (Fig. 3).

Diffusion-weighted imaging (DWI) is able to delineate malignant lesions as hyperintense areas with excellent tissue contrast, and also to provide quantitative measurements of apparent diffusion coefficient (ADC) values [11]. Our study showed DWI to have a sensitivity of 93% and a specificity of 81% for the presence of leiomyosarcomas. Tamai et al. [12] reported significant differences in mean ADC values of LMS compared with normal myometrium and degenerated leiomyomas, even though the SI on DWI between cellular leiomyomas and LMS overlapped, which can be explained by increased cellularity. Namimoto et al. [11] showed that overlap in ADC values between LMS and ordinary leiomyomas (attributed to the "T2 blackout effect," i.e., hypointensity on DWI caused by hypointensity on T2-weighted images) could be resolved with the evaluation of tumor-myometrium contrast ratio on T2-weighted images and demonstrated that combined DWI and ADC values with T2WI could differentiate benign leiomyomas from LMS. Thomassin-Naggara et al. [14] reported that by combining the analysis of T2

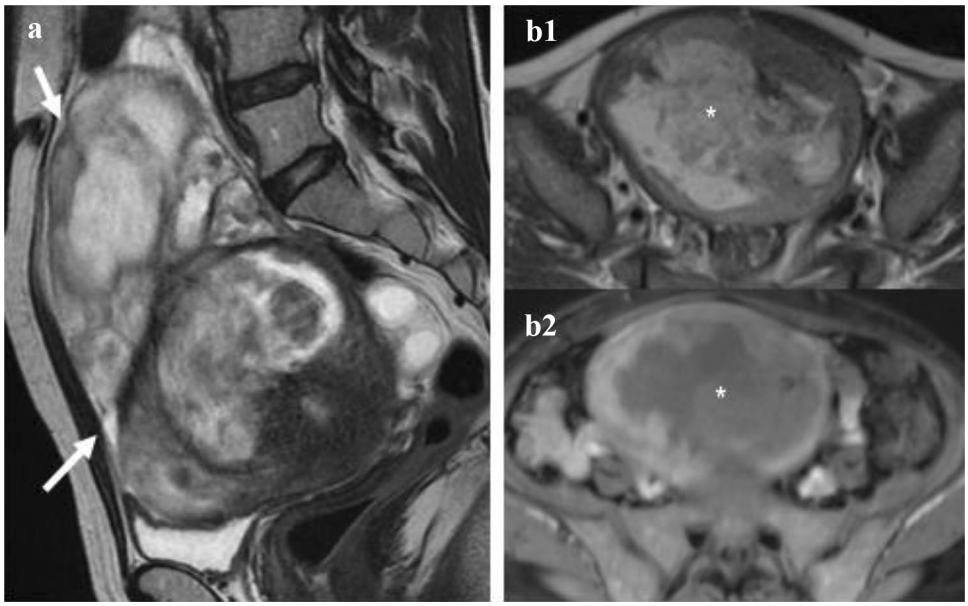

Fig. 3 MRI in a 53-year-old woman shows (**a**) a heterogeneous mass with origin in the uterine myometrium. The tumor demonstrates irregular borders (arrows) and more than 50% of hyperintensity on T2WI (**a**; **b1**). After gadolinium administration (**b2**) central unenhanced areas can be seen representing necrosis (asterisk)

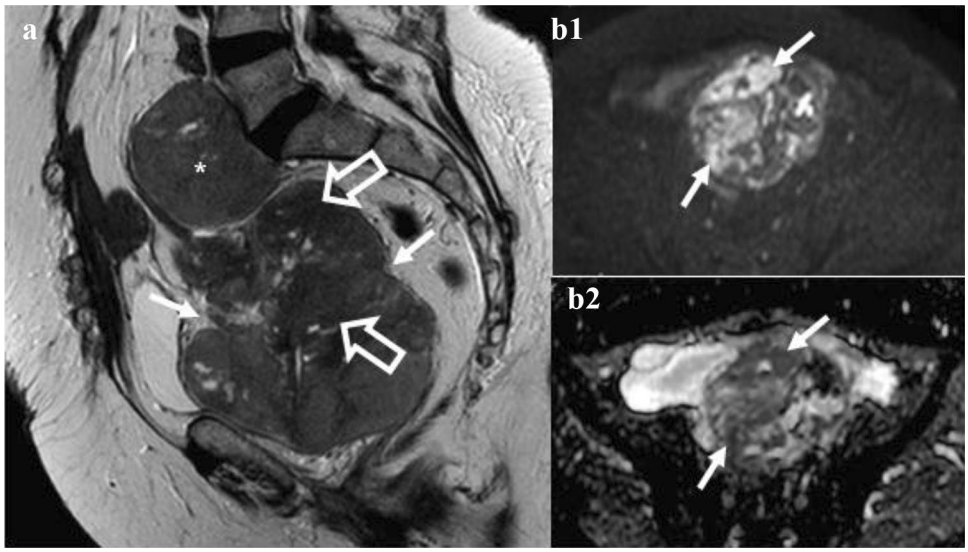

Fig. 4 MRI in a 56-year-old woman shows a heterogeneous uterine mass, with lobulated borders (arrows), T2 dark areas (open arrow), and lumbar lymphadenopathies (asterisk) on sagittal T2WI (**a**). On axial DWI at b1000 (**b1**) the mass demonstrates hyperintensity (arrow) with correspondent low signal on ADC (**b2**), evincing its high cellularity

signal intensity, b1000 images and ADC map, MRI achieved 92.4% accuracy in distinguishing benign and uncertain or malignant myometrial tumors. We also found that the presence of high signal intensity on b1000 images, and low ADC values ($\leq 0.82 \times 10^{-3}$ m^2/s) in patients with tumors showing hyperintensity on T2, could help differentiate between ALM and LMS (Fig. 4). Therefore, the use of DWI must be recommended when evaluating myometrial lesions showing high signal intensity on T2-WI to distinguish between ALM and LMS [25].

Goto et al. found that viable portions of LMS rapidly enhanced on early post-contrast imaging (40–60 s), whereas degenerated leiomyomas typically did not. Because both enhance in later phases, it is essential to include in our study early post-contrast imaging in the dynamic MRI protocol [28]. Furthermore, they suggested that combining dynamic MRI findings with elevated levels of serum lactate dehydrogenase (LDH) and LDH isoenzyme 3 (non-specific tumor markers of LMS) could be helpful in the pre-operative diagnosis of LMS. Most recently, Sato et al. recommended using a combination of diffusion-weighted imaging signal intensity and apparent diffusion coefficient values to stratify patients at high risk of LMS, with high risk lesions having intermediate to high signal on diffusion-weighted imaging and low apparent diffusion coefficient values of $< 1.1 \times 10^{-3}$ mm^2/s) [10]. Similarly, Thomassin-Naggara et al. created a model using high b-value diffusion-weighted imaging signal intensity, high T2-signal intensity, and low apparent diffusion coefficient values to accurately categorize 92% of the tumors in their study as uncertain malignant potential or malignant

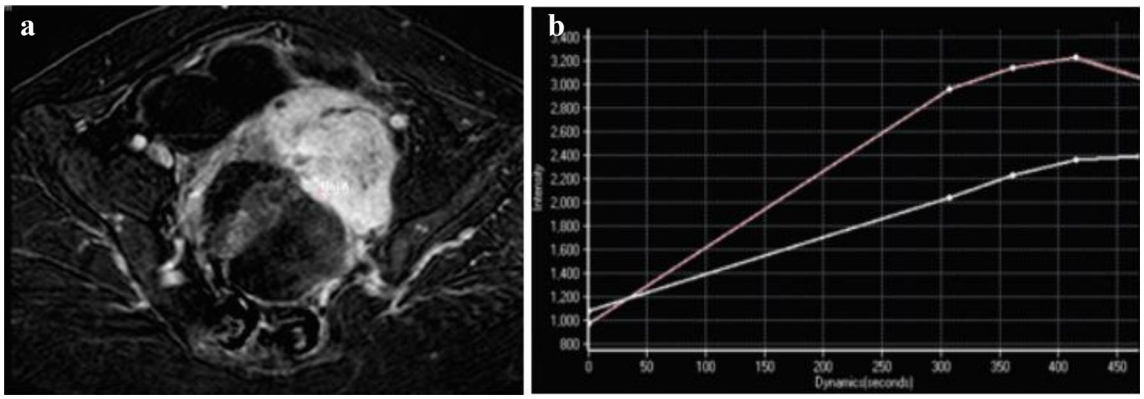

Fig. 5 47-year-old woman with LMS. Axial T1FS after gadolinium administration **a** shows hyperenhancement of the tumor, compared with the myometrium. A ROI was placed on the external myometrium and in the most enhancing part of the tumor (not shown in the image). DCE curve **b** demonstrates rapid enhancement of the tumor (pink curve) compared with the myometrium (grey curve) and latter washout, corresponding to a type 3 curve, which reflect the hypervascular character of the tumor

[14]. Our study is in agreement with previous literature as we also found the presence of hyperenhancement of the tumor compared with the normal myometrium and central unenhanced areas on post-contrast imaging to be related to the presence of a malignant histology, with a sensitivity of 70% and 85% and a specificity of 76% and 85%, respectively. However, unlike Thomassin-Naggara et al. our study found that the presence of rapid enhancement on dynamic contrast images followed by rapid washout toward the latter part of the study (type 3 curve) was associated with the presence of LMS ($p = 0.01$) with a positive predictive value of 93% (Fig. 5).

While all these features are helpful and give diagnostic guidance, currently there are no pre-operative test (clinical or imaging) that can exclude a LMS with certainty [13].

Our study had some limitations. First, the prevalence of atypical mesenchymal neoplasms in our sample is much higher than in the normal population, introducing selection bias. However, we chose our sample to include ALM that were difficult to diagnose and were a cause of misdiagnosis, which represented the sample of cases where our results are applicable and thus ensuring accurate image pathology correlation.

Furthermore, our inter-observer agreement was based on the comparison of the report previously done and the analysis of one reader from the same institution with less sub-specialty training. However, both readers had a common exposure to a large volume of gynecologic oncologic examinations at a tertiary care cancer center and there was an almost perfect agreement for most of the features analyzed.

In summary, we identified that the presence irregular borders, "T2 dark" areas, central, high signal on b1000 DWI, ADC value lower than 0.82, hyperenhancement of the tumor relative to the myometrium on post-contrast images, type 3 enhancing curve on DCE demonstrated strong statistical association with LMS and found that their presence could accurately distinguish LMS from ALM. The presence of irregular borders and central necrotic areas were proven to predict a malignant histology. Prospective studies are needed to externally validate our results.

References

1. Bolan C, Caserta MP (2016) MR imaging of atypical fibroids. Abdom Radiol (NY) 41 (12):2332-2349. https://doi.org/10.1007/s00261-016-0935-0
2. Ryan GL, Syrop CH, Van Voorhis BJ (2005) Role, epidemiology, and natural history of benign uterine mass lesions. Clin Obstet Gynecol 48 (2):312-324
3. Rha SE, Byun JY, Jung SE, Lee SL, Cho SM, Hwang SS, Lee HG, Namkoong SE, Lee JM (2003) CT and MRI of uterine sarcomas and their mimickers. AJR Am J Roentgenol 181 (5):1369-1374. https://doi.org/10.2214/ajr.181.5.1811369
4. Arleo EK, Schwartz PE, Hui P, McCarthy S (2015) Review of Leiomyoma Variants. AJR Am J Roentgenol 205 (4):912-921. https://doi.org/10.2214/ajr.14.13946
5. Schwartz LB, Zawin M, Carcangiu ML, Lange R, McCarthy S (1998) Does pelvic magnetic resonance imaging differentiate among the histologic subtypes of uterine leiomyomata? Fertil Steril 70 (3):580-587
6. Owen C, Armstrong AY (2015) Clinical management of leiomyoma. Obstet Gynecol Clin North Am 42 (1):67-85. https://doi.org/10.1016/j.ogc.2014.09.009
7. Ueda H, Togashi K, Konishi I, Kataoka ML, Koyama T, Fujiwara T, Kobayashi H, Fujii S, Konishi J (1999) Unusual appearances of uterine leiomyomas: MR imaging findings and their histopathologic backgrounds. Radiographics 19 Spec No:S131-145. https://doi.org/10.1148/radiographics.19.suppl_1.g99oc04s131
8. Cornfeld D, Israel G, Martel M, Weinreb J, Schwartz P, McCarthy S (2010) MRI appearance of mesenchymal tumors of the uterus. Eur J Radiol 74 (1):241-249. https://doi.org/10.1016/j.ejrad.2009.03.005
9. Tanaka YO, Nishida M, Tsunoda H, Okamoto Y, Yoshikawa H (2004) Smooth muscle tumors of uncertain malignant potential

and leiomyosarcomas of the uterus: MR findings. J Magn Reson Imaging 20 (6):998-1007. https://doi.org/10.1002/jmri.20207
10. . Sato K, Yuasa N, Fujita M, Fukushima Y (2014) Clinical application of diffusion-weighted imaging for preoperative differentiation between uterine leiomyoma and leiomyosarcoma. Am J Obstet Gynecol 210 (4):368 e361-368 e368. https://doi.org/10.1016/j.ajog.2013.12.028
11. Namimoto T, Yamashita Y, Awai K, Nakaura T, Yanaga Y, Hirai T, Saito T, Katabuchi H (2009) Combined use of T2-weighted and diffusion-weighted 3-T MR imaging for differentiating uterine sarcomas from benign leiomyomas. Eur Radiol 19 (11):2756-2764. https://doi.org/10.1007/s00330-009-1471-x
12. Tamai K, Koyama T, Saga T, Morisawa N, Fujimoto K, Mikami Y, Togashi K (2008) The utility of diffusion-weighted MR imaging for differentiating uterine sarcomas from benign leiomyomas. Eur Radiol 18 (4):723-730.. https://doi.org/10.1007/s00330-007-0787-7
13. Lakhman Y, Veeraraghavan H, Chaim J, Feier D, Goldman DA, Moskowitz CS, Nougaret S, Sosa RE, Vargas HA, Soslow RA, Abu-Rustum NR, Hricak H, Sala E (2017) Differentiation of Uterine Leiomyosarcoma from Atypical Leiomyoma: Diagnostic Accuracy of Qualitative MR Imaging Features and Feasibility of Texture Analysis. Eur Radiol 27 (7):2903-2915. https://doi.org/10.1007/s00330-016-4623-9
14. Thomassin-Naggara I, Dechoux S, Bonneau C, Morel A, Rouzier R, Carette MF, Darai E, Bazot M (2013) How to differentiate benign from malignant myometrial tumours using MR imaging. Eur Radiol 23 (8):2306-2314. https://doi.org/10.1007/s00330-013-2819-9
15. Sahdev A, Sohaib SA, Jacobs I, Shepherd JH, Oram DH, Reznek RH (2001) MR imaging of uterine sarcomas. AJR Am J Roentgenol 177 (6):1307-1311. https://doi.org/10.2214/ajr.177.6.1771307
16. Tasaki A, Asatani MO, Umezu H, Kashima K, Enomoto T, Yoshimura N, Aoyama H (2015) Differential diagnosis of uterine smooth muscle tumors using diffusion-weighted imaging: correlations with the apparent diffusion coefficient and cell density. Abdom Imaging 40 (6):1742-1752. https://doi.org/10.1007/s00261-014-0324-5
17. Rigby AS (2000) Statistical methods in epidemiology. v. Towards an understanding of the kappa coefficient. Disabil Rehabil 22 (8):339-344
18. Wallach EE, Vlahos NF (2004) Uterine myomas: an overview of development, clinical features, and management. Obstet Gynecol 104 (2):393-406. https://doi.org/10.1097/01.aog.0000136079.62513.39
19. Stewart EA (2015) Clinical practice. Uterine fibroids. N Engl J Med 372 (17):1646-1655. https://doi.org/10.1056/nejmcp1411029
20. Pron G (2015) Magnetic Resonance-Guided High-Intensity Focused Ultrasound (MRgHIFU) Treatment of Symptomatic Uterine Fibroids: An Evidence-Based Analysis. Ont Health Technol Assess Ser 15 (4):1-86
21. Pritts EA, Vanness DJ, Berek JS, Parker W, Feinberg R, Feinberg J, Olive DL (2015) The prevalence of occult leiomyosarcoma at surgery for presumed uterine fibroids: a meta-analysis. Gynecol Surg 12 (3):165-177. https://doi.org/10.1007/s10397-015-0894-4
22. Pron G (2006) New uterine-preserving therapies raise questions about interdisciplinary management and the role of surgery for symptomatic fibroids. Fertil Steril 85 (1):44-45; discussion 48-50. https://doi.org/10.1016/j.fertnstert.2005.09.014
23. Wu TI, Yen TC, Lai CH (2011) Clinical presentation and diagnosis of uterine sarcoma, including imaging. Best Pract Res Clin Obstet Gynaecol 25 (6):681-689. https://doi.org/10.1016/j.bpobgyn.2011.07.002
24. Matsuda M, Ichimura T, Kasai M, Murakami M, Kawamura N, Hayashi T, Sumi T (2014) Preoperative diagnosis of usual leiomyoma, atypical leiomyoma, and leiomyosarcoma. Sarcoma 2014:498682. https://doi.org/10.1155/2014/498682
25. Santos P, Cunha TM (2015) Uterine sarcomas: clinical presentation and MRI features. Diagn Interv Radiol 21 (1):4-9. https://doi.org/10.5152/dir.2014.14053
26. Hricak H, Tscholakoff D, Heinrichs L, Fisher MR, Dooms GC, Reinhold C, Jaffe RB (1986) Uterine leiomyomas: correlation of MR, histopathologic findings, and symptoms. Radiology 158 (2):385-391. https://doi.org/10.1148/radiology.158.2.3753623
27. Murase E, Siegelman ES, Outwater EK, Perez-Jaffe LA, Tureck RW (1999) Uterine leiomyomas: histopathologic features, MR imaging findings, differential diagnosis, and treatment. Radiographics 19 (5):1179-1197. https://doi.org/10.1148/radiographics.19.5.g99se131179
28. Goto A, Takeuchi S, Sugimura K, Maruo T (2002) Usefulness of Gd-DTPA contrast-enhanced dynamic MRI and serum determination of LDH and its isozymes in the differential diagnosis of leiomyosarcoma from degenerated leiomyoma of the uterus. Int J Gynecol Cancer 12 (4):354-361

Publisher's Note Springer Nature remains neutral with regard to jurisdictional claims in published maps and institutional affiliations.